EM Implosion Memos

Memo 25

February 2009

EM Probe Design for an Electromagnetic Focusing Lens

Serhat Altunc, Carl E. Baum, C. Jerald Buchenauer, Christos G. Christodoulou and Edl Schamiloglu

University of New Mexico
Department of Electrical and Computer Engineering
Albuquerque New Mexico 87131

Abstract

This paper has provided a discussion on EM probe design for subhundredpicosecond pulses. Some preliminary experimental results and rough analytical spot size analyses are presented.

1 Introduction

Experimental setups using a 60^o four-arm prolate-spheroidal IRA (PSIRA or ΨRA) are used to obtain better focusing at the second focus of a ΨRA for skin cancer treatment [1]. The dimensions of these experiments are based on [2-6]. Figure 1 presents the ΨRA geometry and lens geometry. The parameters for this geometry are

$$z_p = 0,\ \ a = .625\ \text{m},\ b = \Psi_0 = .5\,\text{m},\ z_0 = .375\,\text{m}\ , \tag{1}$$

where z_p is the z-coordinate of the truncation plane, a and b are the two radii for the prolate-spheroidal reflector and z_0 is the focal distance. The basic design considerations of a variable ε_r lens with constant wavelength to cross section ratio are discussed. Basic design considerations, numerical results and preliminary experimental results of this lens are discussed in [7-9]. This paper deals with a half spherical lens design with subsequent layers.

We have designed a lens with constant wavelength to cross section ratio as ε_r varies. Therefore r/λ is not a function of r and one can easily define

$$\begin{aligned} &\varepsilon_r(r) \equiv (r_{max}/r)^2 \qquad r \geq r_0, \\ &\varepsilon_{r\,max} \equiv (r_{max}/r_0)^2 \quad r \leq r_0 \end{aligned} \tag{2}$$

where r is the radius of the lens, r_{max} is the radius of the outer shell and r_0 is the constant center radius.

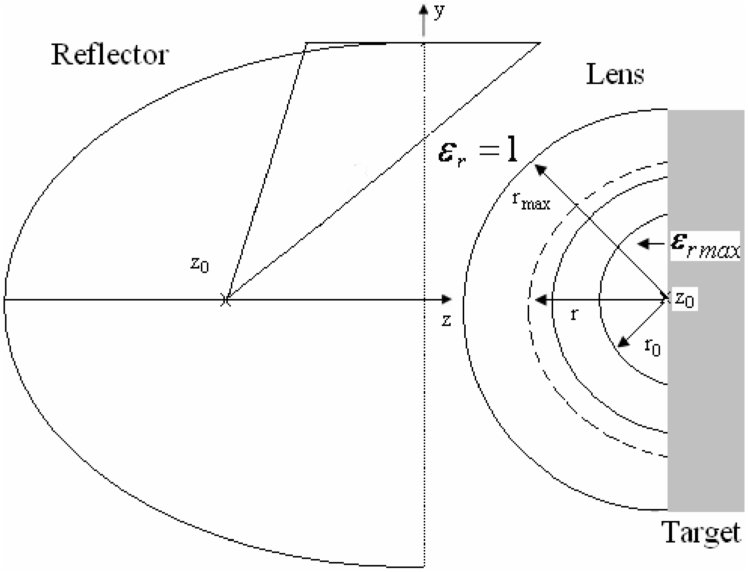

Figure 1. IRA and Lens Geometry.

2 Experiment and Probe Design

The experimental results are normalized to 1 Volt differential input and t_{mr} (maximum rate of rise) is used as t_{δ}, the rise time of the ramp rising step excitation, to compare our experimental results with analytical and numerical results. For a step like $f(t)$, the t_{mr} is

$$t_{mr} = f_{max} \Big/ \left.\frac{df}{dt}\right|_{max} . \tag{3}$$

Figure 2 presents the 60^{o} four-feed arm ΨRA with lens at the second focal point. The initial experiments use four essential components: a ΨRA with feed arms, sampling-oscilloscope with a 2 mm diameter B-dot probe, pulse generator and spherical lens with five layers. The output of the step generator has a 45-ps rise time, and 10 V amplitude.

Figure 3 shows the geometry of the log periodic lens with 5 layers for $\varepsilon_{r\,max} = 9$, target and B-dot probe with 2 mm diameter.

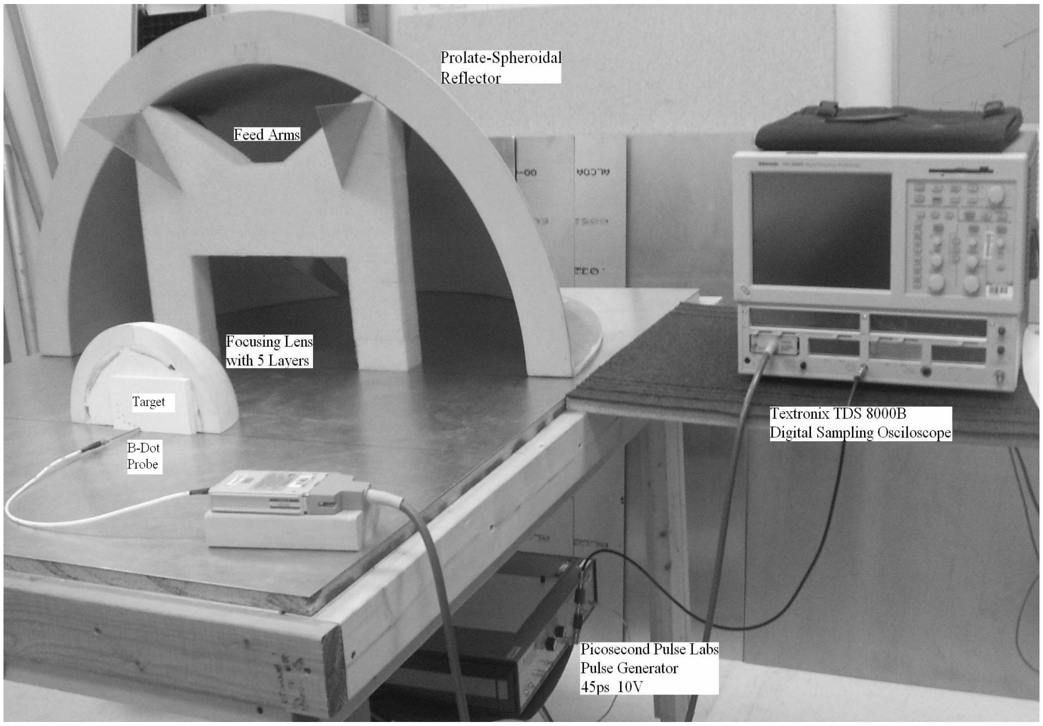

Figure 2. Experimental setup for 60^{o} four- arms ΨRA and lens.

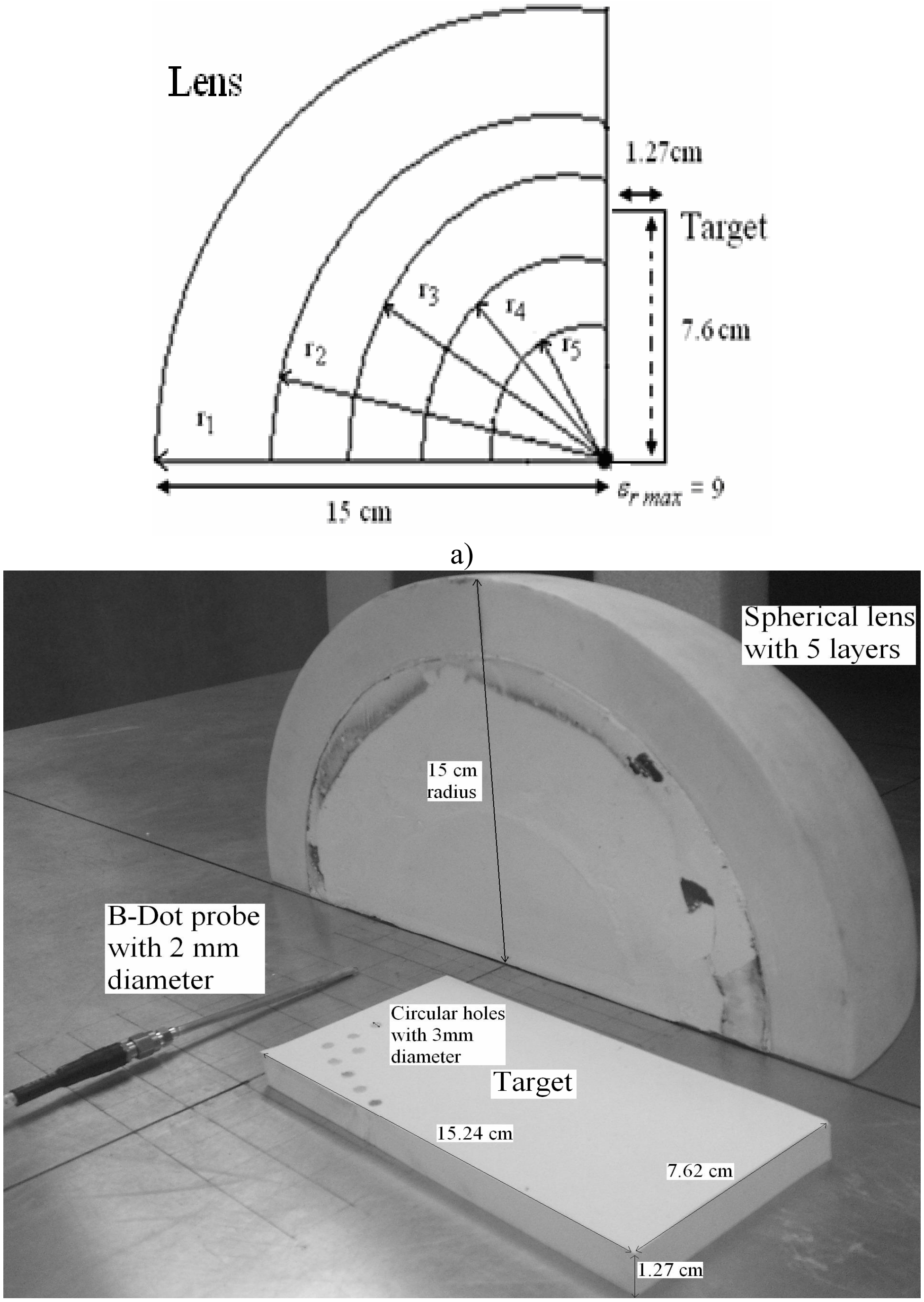

a)

b)

Figure 3 a)Log -periodic lens for $\varepsilon_{r\,max} = 9$ with 5 layers and target side-view b) spherical lens with 5 layers, B-dot probe with 2 mm diameter and target (7.62 cmX15.24 cmX1.27 cm) .

2.1 Probe Design

One of the most challenging parts of this experiment is probe design. We should design a D-dot or B-dot probes to measure the subnanosecond pulse pulse. These probes should be embedded at the second focus between lens and target. Figure 4 is devoted to the possible D-dot or B-dot probes design. The gap and wire part of the B-dot probe provide a lower inductance for B-dot probe.

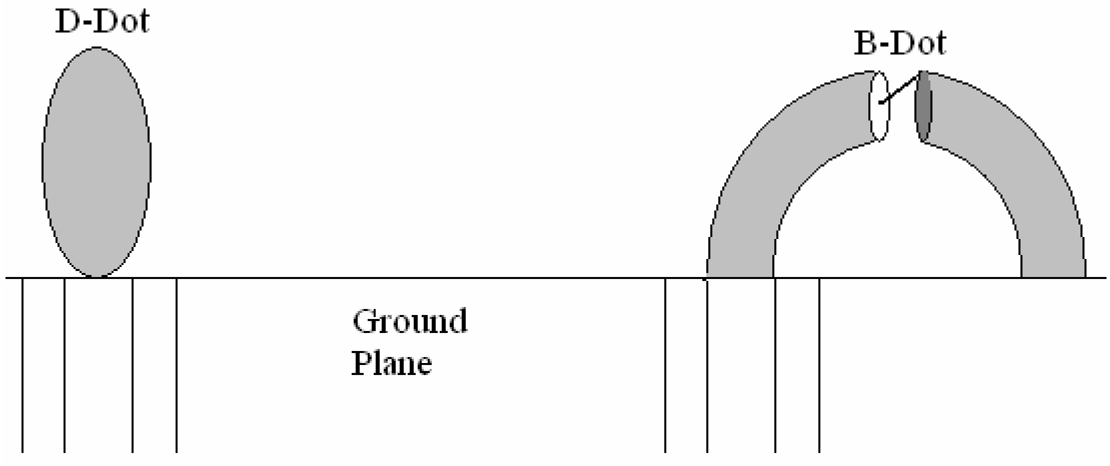

Figure 4 D-dot and B-dot probes located at the second focal point.

While designing a B-dot probe, one should satisfy

$$2L/R < t_{mr} \text{ , times of interest} \tag{4}$$

Where L is the sensor inductance and $R = 50\,\Omega$ is the load resistance [8]. In addition, the sensor size (transit times) should be small compared to times of interest [9].

These sensors will be embedded at the second focal point. We are planning to use a fast D-dot and B-dot probes between the lens and target. The fast D-dot probe should be contact with $\varepsilon_{r\,target}$ medium and the ε_r value should be the same through the spot size region.

2.2 Field Amplitude and Spot Size Analyses

One of the most important features of this lens is obtaining $\varepsilon_{r\,target}^{1/2}$ times smaller spot sizes. This will eliminate the damage on the healthy cells and provide higher-amplitude EM pulses in a smaller space and better match the wave into the target. Given that the impulse has some small width $t_\delta = 100$ ps, the maximum fields will exist in some small region around z_0. The fast D-dot probe, however, can resolve the pulse to be about 30 ps, which implies a three times higher field amplitude. For the larger pulse we can make a rough estimate of spot sizes as in [4]. The pulse width to define a boundary spot with respect to Ψ and z is

$$t_{\Psi} = t_z = 2t_{\delta} = 200\,\text{ps}\,. \tag{5}$$

Spot sizes are calculated analytically in [4] as

$$|\Delta z| = 2\,[1 - z_0/a]^{-1} ct_{\delta} = 15\,\text{cm}, \Delta\Psi = \frac{a}{b} ct_{\delta} = 3.75\,\text{cm}\,. \tag{6}$$

We have observed acceptable agreement with equation (6) and our preliminary experimental results. Figure 5 shows the shrinkage in the spot size along y-axis for the experimental setups with lens and without lens. One can see from figure 5 that the field amplitude is down by the half of the focal waveform amplitude at

$$\begin{aligned} &y = 3.75\,\text{cm} && (\text{with lens}) \\ &y = 3.75/\varepsilon_{r\,target}^{1/2} = 3.75/9^{1/2} = 1.25\,\text{cm} && (\text{without lens}) \end{aligned} \quad . \tag{7}$$

As seen from (6), if we use a faster probe, we should obtain a smaller spot size. We have used a D-dot probe which has a $t_{mr} = 30\,\text{ps}$. One can calculate the analytical spot size from (6)

$$\Delta\Psi = \frac{a}{b} ct_{\delta} \approx 1.25\,\text{cm} \tag{8}$$

Figure 6 presents the normalized E-Field amplitude variation through the y-axis for slow D-dot probe ($t_{mr} = 100\,\text{ps}$) and fast D-dot probe($t_{mr} = 30\,\text{ps}$) which has an acceptable agreement with (8).

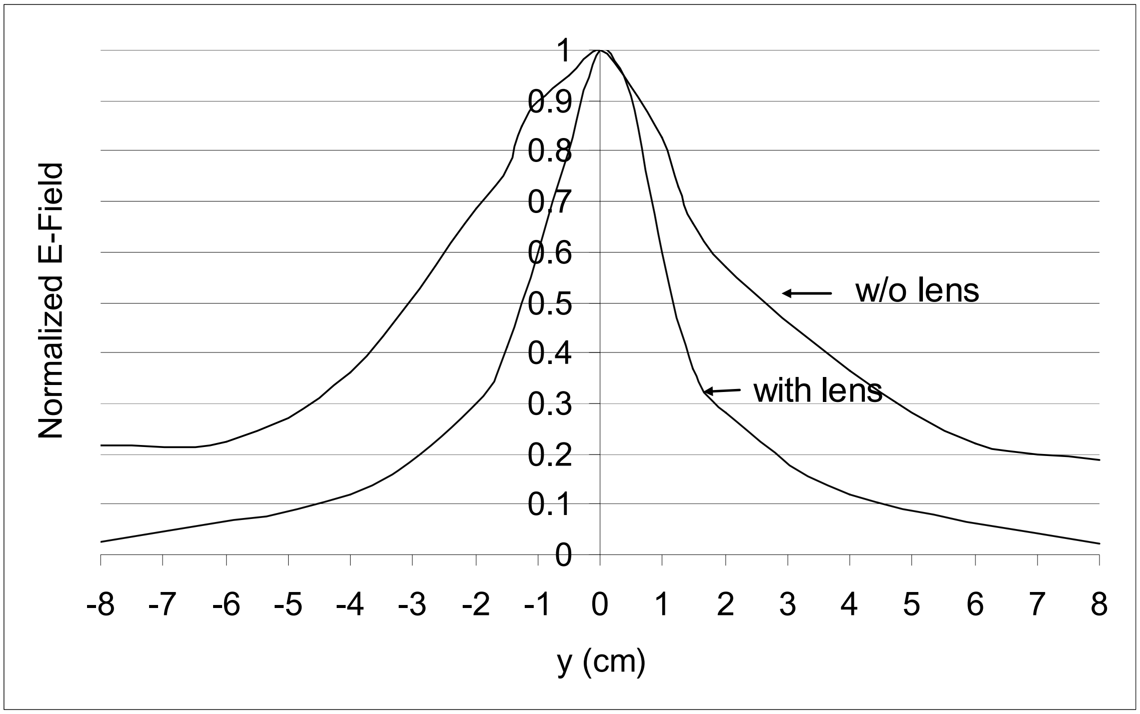

Figure 5. Shrinkage of the spot size for fast B-dot probe($t_{mr} \cong 30\,\text{ps}$)

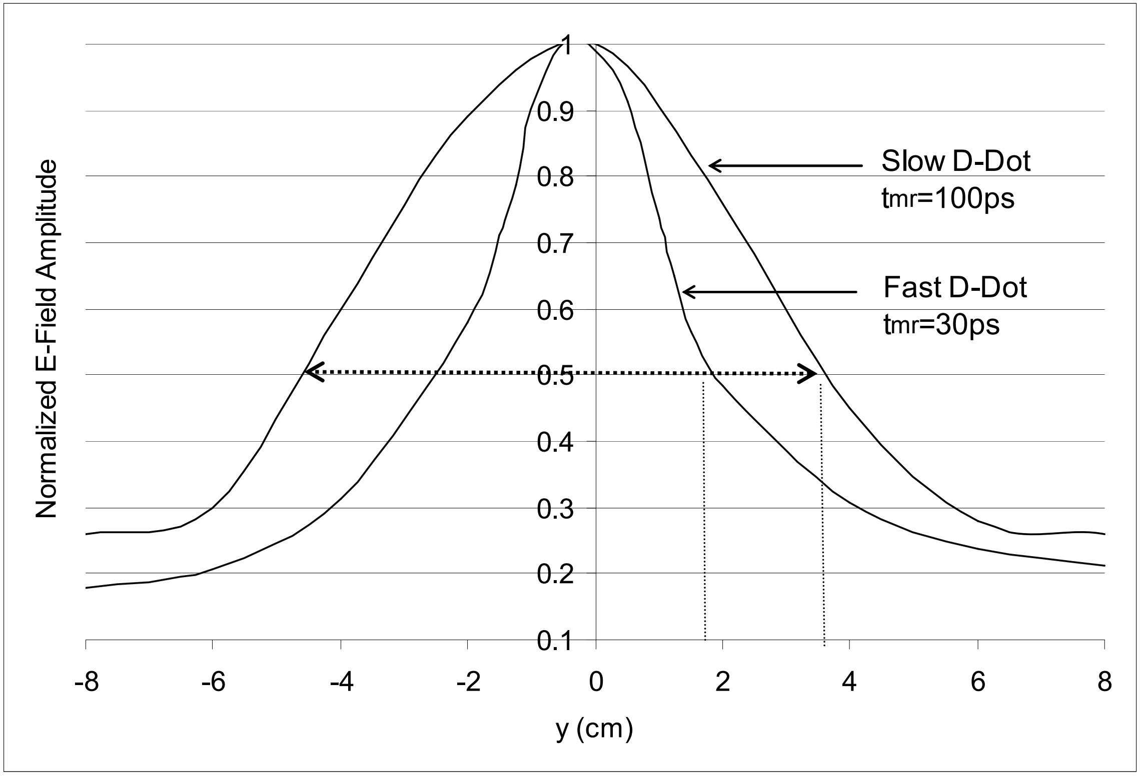

Figure 6 Normalized E-Field Amplitude variation through y-axis for slow D-dot probe($t_{mr} \cong 100\,\text{ps}$) and fast D-dot probe($t_{mr} \cong 30\,\text{ps}$).

Conclusion

This paper discusses a new type of a subnanosecond focusing lens for a ΨRA which has been started to use as an noninvasive pulse delivery system for skin-cancer treatment in the near field region. This lens will reduce the damage to the tissue layers surrounding the target and skin [8]. We have discussed D-dot and B-dot probes design for subnanosecond pulses. Preliminary experimental results and analytical spot size analyses are presented.

References

[1] K. H. Schoenbach, R. Nuccitelli, and S. J. Beebe, “Zap,” IEEE Spectrum, pp. 20–28, 1980.

[2] Altunc, S., C. E. Baum, C. G. Christodoulou, E. Schamiloglu, and C. J. Buchenauer, “Focal waveforms for various source waveforms driving a prolate-spheroidal impulse radiating antenna (IRA)”, Radio Sci., 43, p. RS4S13, 2008.

[3] C. E. Baum, “Focal waveform of a prolate spheroidal IRA,” Radio Sci., vol. 42, no. 6, p. RS6S27, 2007.

[4] C.E. Baum, S. Altunc, C.G. Christodoulou and E. Schamiloglu, “Electromagnetic implosion using an Array,” IEEE Trans. Plasma Science, Vol. 36, pp. 757-763, 2008

[5] C. E. Baum, “Addition of a lens before the second focus of apProlate-spheroidal IRA”, Sensor and Simulation Note 512, 2006.

[6] S. Altunc and C. E. Baum, “Lens design for a prolate spheroidal IRA”, Sensor and Simulation Note 525, 2007.

[7] Altunc S., C.E. Baum, C. G. Christodoulou and E. Schamiloglu “Design of a special dielectric lens for concentrating a subnanosecond electromagnetic pulse on a biological target,” under review, IEEE Transactions on Dielectrics and Electrical Insulation .

[8] C. E. Baum, “Parameters for some electrically small electromagnetic sensors”, Sensor and Simulation Note 38, 1967.

[9] C. E. Baum, “Maximizing frequency response of a $\dot{B}$ loop”, Sensor and Simulation Note 8, 1964.